

Response to reviewer #1 (Dr. S. Paolo)

- I agree with Scesi's comment and I found quite obscure the physical description of the site given in Section 2, mainly with reference to the spatial interaction of wells with joints and faults. The maps and the section reported in Figure from 1 to 3, as well as the information given in the text, are inadequate to understand the scale of the problem. In other words I'm unable to understand how (in a statistical sense) the boreholes are crossed by fractures and I think that this fact is of paramount relevance in the analysis. This is confirmed by the Authors themselves that at page 2000 state: "The GRF model is therefore applicable to the CGF because it is homogeneous and isotropic based on the field description and anisotropic analysis." The latter statement is based on the analysis of five sets of well combination (Table 2), but "the directions in sets 4 and 5 are inconsistent with the direction of prominent set of joints in Fig. 4" (page 2000) and for this reason only the results of sets from 1 to 3 are considered as valid. If the physical description can decide whether the results of the computations are to be accepted or rejected (I generally agree with this attitude), I think that it must be clear without any doubt.

Reply:

- Sorry for the confusing directions of fault and joints. The direction "NE-SW" in the following texts are typos: "...numerous trust faults that essentially trend parallel to the bedding (NE-SW) and ..." (line 21, p. 1993) and "the most convex of the NE-SW trust..." (line 26, P. 1993). According to the geological analysis by Tseng (1978), the fault and joints should have "NW-SE" direction. Those texts are therefore modified as "...numerous trust faults that essentially trend parallel to the bedding (NW-SE) and ..." and "the most convex of the NW-SE trust...". In addition, the Chingshuihsi fault has NW-SE direction and thus the text "There is a normal, N-S striking Chingshuihsi fault..." is modified as "There is a normal, NW-SE striking Chingshuihsi fault..." (line 25, p. 1993). Moreover, according to Tseng (1978), the strike of most prominent set of joints is $N25^{\circ} W$ and $N40^{\circ} W$ dips between $75^{\circ} - 90^{\circ}$ to SW and the strike of the Chingshuihsi fault is about $N30^{\circ} W$ and $N35^{\circ} W$. The strikes of the most important sets of the joints and fault are almost parallel. Unfortunately, Tseng (1978) did not provide the dip direction and the azimuth of the fault. From the analysis of geologic, gravity, and magnetotelluric data by Tong et al. (2008), the fault system is $N21^{\circ} W$ and dips 80° to NE. We adopt this result and add it in the manuscript since it is integrated by many geophysics data and borehole information.

- Moreover I suggest to give a simple recall of the Papadopulous method, being the “Proceeding of the Dubrovnik Symposium on the Hydrology of Fractured Rocks, International Association of Scientific Hydrology, 21–31, 1965” substantially unavailable to most the readers.

Reply:

- Thanks for the suggestion. The following text is added in the revised manuscript: The anisotropic analysis is made based on the model of Papadopulous (1965) as follows

$$T_{xx} \frac{\partial^2 s}{\partial x^2} + 2T_{xy} \frac{\partial^2 s}{\partial x \partial y} + T_{yy} \frac{\partial^2 s}{\partial y^2} + Q\delta(x)\delta(y) = S \frac{\partial s}{\partial t}$$

where T represents the transmissivity, S represents the storage coefficient, and s is the drawdown. Four sets of combination of three wells from the four observation wells and one set of composite wells as shown in Table A are analyzed using Papadopulous’ model with known coordinates of the well locations. The coordinates of the observation wells from pumping well 16T are (-89 m, 150.65 m) for 4T, (-79 m, 289 m) for 9T, (55 m, 71 m) for 12T and (260 m, -200 m) for 14T. The angles for the wells can also be estimated from the coordinates of the well locations. The results of anisotropic analysis are also shown in Table 2 with $T_{\xi\xi}$ and $T_{\eta\eta}$ defined as the major and minor principal directional components of the transmissivity tensor, respectively and θ defined as the angle between the x-axis and the direction of the major principal transmissivity. The defintions of $T_{\xi\xi}$, $T_{\eta\eta}$ and θ are as following

$$T_{\xi\xi} = \frac{1}{2} \left\{ (T_{xx} + T_{yy}) + \left[(T_{xx} - T_{yy})^2 + 4T_{xy}^2 \right]^{1/2} \right\}$$

$$T_{\eta\eta} = \frac{1}{2} \left\{ (T_{xx} + T_{yy}) - \left[(T_{xx} - T_{yy})^2 + 4T_{xy}^2 \right]^{1/2} \right\}$$

and

$$\theta = \arctan \left(\frac{T_{\xi\xi} - T_{xx}}{T_{xy}} \right)$$

- In any case, the aforementioned aspects were widely discussed in the comment by L. Scesi, thus I prefer to spend some words about the joined GRF and SA analysis. All the results (dimensionality n , transmissivity T , and storativity S) are reported in Table 3, with the standard error of estimate (SEE) as a function of the distance between the pumping well and the observation well. From my point of

view the results depend on: i) the choice of the objective function (eq. 6 of page 1997), and ii) the choice of the temperature reduction factor, assumed “constant and smaller than one” (page 1999). With reference to the point i), I would like to see the effects related to a different formulation of the objective function, as an example by weighing in a different manner early and late time drawdown data and/or by defining as objective function the absolute value instead of the square of the difference between observed and predicted head. This may give an idea of the robustness of the results, which show great differences in the parameter n , T , and S even if the drawdown behavior is quite similar. This situation is shown in Fig. 5 (cases a, b, and d), where the estimated drawdown using a general GRF solution and the Theis (GRF with fixed $n=2$) solution are compared.

Reply:

- It is important to choose appropriate weights in the objective function to estimate the hydraulic parameters and flow dimension. We first analyze the sensitivity of T , S and n to investigate the relationships between the drawdown data and the estimated parameters. From Figure as shown below, the drawdown is sensitive to the hydraulic parameters T and S and flow dimension n except at the early period of the pumping. In addition, the sensitivity of T , S and n are continuously increased through the end of the pumping. Two approaches are commonly used to assign the weights (Berthouex and Brown, 2002, pp. 327-331). The first is to assume that the weights are inversely proportional to the variance of each observation ($w_i = 1/\sigma_i^2$). However, it is impossible to calculate the variance without replicates. Thus, another approach is to assign the weights are inversely proportional to the value of independent variable. Since the sensitivity results indicate that the late-time drawdown data are more critical than the early-time drawdown data, we use the weight $w_i = time_i / \sum_{i=1}^{11} time_i$ which reflects that the late-time data is more important than the early-time data. Tables A and B listed below show the estimated parameters using unweighted and weighted objective function, respectively. Apparently, the estimated parameters using weighted objective function are different from those using unweighted objective function because of the different weights. However, the estimated parameters are slightly different and the results also demonstrate that the flow dimension increases with the distance between the pumping well and the observation well.

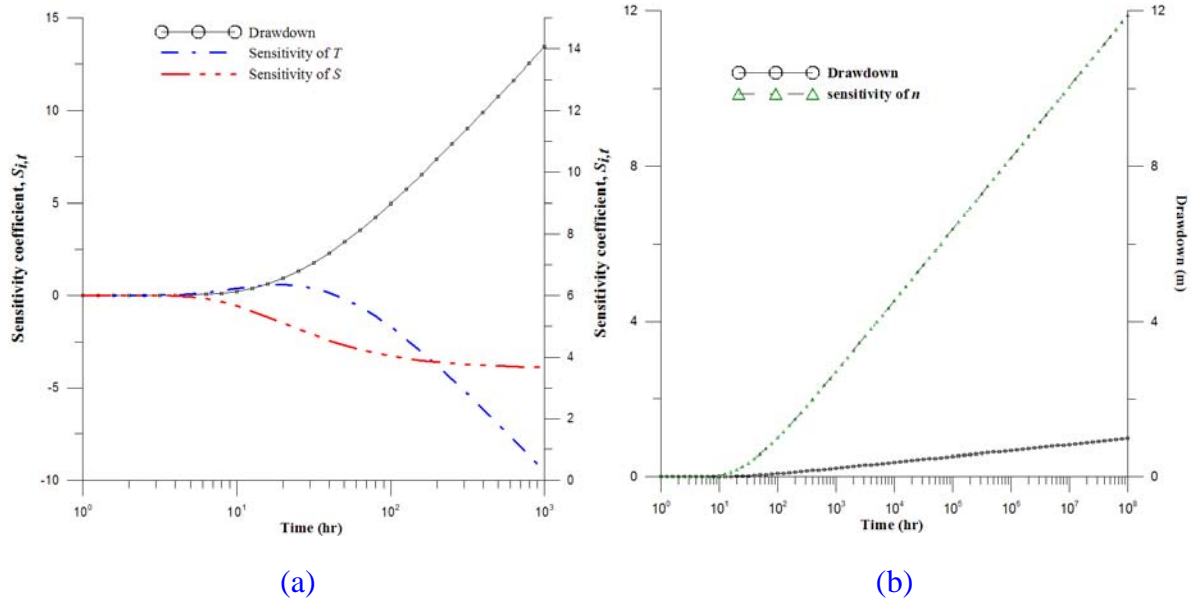


Figure a. The time-drawdown data and the sensitivities of the (a) hydraulic parameters T and S and (b) the flow dimension n

Table A. The estimated parameters using unweighted objective function

Observation well	r (m)	Estimated hydrogeologic parameters			SEE
		n	T ($m^2 \text{min}^{-1}$)	S	
12T	90	1.31	99.9×10^3	9.99×10^3	0.38
4T	175	1.95	48.9×10^3	5.13×10^3	0.35
9T	300	2.11	71.2×10^3	3.64×10^3	0.44
14T	330	2.27	96.0×10^3	6.54×10^3	0.57

Table B. The estimated parameters using weighted objective function

Observation well	r (m)	Estimated hydrogeologic parameters			SEE
		n	T ($m^2 \text{min}^{-1}$)	S	
12T	90	1.31	96.6×10^3	9.97×10^3	0.108
4T	175	1.51	99.5×10^3	5.15×10^3	0.089
9T	300	2.15	93.3×10^3	4.62×10^3	0.115
14T	330	2.23	75.3×10^3	5.22×10^3	0.140

- Moreover, as reported in “Press et al., Numerical Recipes, The Art of Scientific Computing, 2nd edition, 1992”, the essence of the minimization process is slow cooling and, even at low temperature, there is a “chance for the analyzed system to get out of a local energy minimum in favor of finding a better, more global, one”. The thermodynamic analogy is remarked by the Authors themselves, although they don’t show any result of a (quite mandatory) sensitivity analysis

about the temperature reduction factor. I suggest that this will be done to reasonably ensure about the minimum obtained with the SA method.

Reply:

- For examining the robustness and reliability of SA in parameter identification, Yeh et al. (2007) and Huang et al. (2008) presented the sensitivity analyses of control parameters in SA for the parameter identification. They demonstrated that the temperature reduction factor does not seem to affect the results of the parameter identification. Table C shows the estimated parameters and flow dimension for 4T, 9T, 12T and 14T when the temperature reduction factor R_{Te} varies from 0.50 to 0.90 with 0.05 increments. The results of estimated parameters and flow dimension with three significant digits are all the same for different values of R_{Te} for these wells. These results indicate that the parameter estimation is independent of R_{Te} values in our case.

Table C. The estimated hydrogeologic parameters for 4T, 9T, 12T and 14T using various temperature reduction factor R_{Te}

4T			
R_{Te}	T ($\text{m}^2\text{min}^{-1}$)	S	n
0.50	48.9×10^{-3}	5.13×10^{-3}	1.95
0.55	48.9×10^{-3}	5.13×10^{-3}	1.95
0.60	48.9×10^{-3}	5.13×10^{-3}	1.95
0.65	48.9×10^{-3}	5.13×10^{-3}	1.95
0.70	48.9×10^{-3}	5.13×10^{-3}	1.95
0.75	48.9×10^{-3}	5.13×10^{-3}	1.95
0.80	48.9×10^{-3}	5.13×10^{-3}	1.95
0.85	48.9×10^{-3}	5.13×10^{-3}	1.95
0.90	48.9×10^{-3}	5.13×10^{-3}	1.95
9T			
R_{Te}	T ($\text{m}^2\text{min}^{-1}$)	S	n
0.50	71.2×10^{-3}	3.64×10^{-3}	2.11
0.55	71.2×10^{-3}	3.64×10^{-3}	2.11
0.60	71.2×10^{-3}	3.64×10^{-3}	2.11
0.65	71.2×10^{-3}	3.64×10^{-3}	2.11
0.70	71.2×10^{-3}	3.64×10^{-3}	2.11
0.75	71.2×10^{-3}	3.64×10^{-3}	2.11
0.80	71.2×10^{-3}	3.64×10^{-3}	2.11
0.85	71.2×10^{-3}	3.64×10^{-3}	2.11
0.90	71.2×10^{-3}	3.64×10^{-3}	2.11

12T			
R_{Te}	T ($\text{m}^2\text{min}^{-1}$)	S	n
0.50	99.9×10^{-3}	9.99×10^{-3}	1.31
0.55	99.9×10^{-3}	9.99×10^{-3}	1.31
0.60	99.9×10^{-3}	9.99×10^{-3}	1.31
0.65	99.9×10^{-3}	9.99×10^{-3}	1.31
0.70	99.9×10^{-3}	9.99×10^{-3}	1.31
0.75	99.9×10^{-3}	9.99×10^{-3}	1.31
0.80	99.9×10^{-3}	9.99×10^{-3}	1.31
0.85	99.9×10^{-3}	9.99×10^{-3}	1.31
0.90	99.9×10^{-3}	9.99×10^{-3}	1.31
14T			
R_{Te}	T ($\text{m}^2\text{min}^{-1}$)	S	n
0.50	96.0×10^{-3}	6.54×10^{-3}	2.27
0.55	96.0×10^{-3}	6.54×10^{-3}	2.27
0.60	96.0×10^{-3}	6.54×10^{-3}	2.27
0.65	96.0×10^{-3}	6.54×10^{-3}	2.27
0.70	96.0×10^{-3}	6.54×10^{-3}	2.27
0.75	96.0×10^{-3}	6.54×10^{-3}	2.27
0.80	96.0×10^{-3}	6.54×10^{-3}	2.27
0.85	96.0×10^{-3}	6.54×10^{-3}	2.27
0.90	96.0×10^{-3}	6.54×10^{-3}	2.27

- I'm unable to deduce from Fig. 1 the distances from the pumping well reported in Table 3.

Reply:

The distances between the observation and production wells used in this study are adopted from Fan et al. (2005). The distance between wells corresponds to the distance between pairs of feed zones which are estimated from the locations of 1500 m depth and well bottom according to the well completion data for wells in Chingshui geothermal field (CGF) (see Fan et al. (2005), Table 3, p. 107).

- Why do the Authors spend a large part of the paper to criticize the work by Le Borgne et al. [2004]? The results showed in that paper are not manifestly in contrast with those (quite obvious) presented here. If the scope is to demonstrate that the use of SA is better than the “graphical fitting procedure” adopted by La Borgne, I suggest that the Authors modify the Sections 4.1 by enhancing in the discussion the differences that can be obtained by means of their and other

approaches. In this case an application of a different procedure (the graphical fitting?) on their own data is also required.

Reply:

The reason why we discussed the results in Le Borgne et al. (2004) is that they indicated there is no obvious relation between the flow dimension and the distance from the pumping well while we found that there is an obvious scale-dependent effect in our study. We think that the contradictory results should be clearly explained.

References

- Berthouex, P.M., Brown, L.C. 2002. *Statistics for Environmental Engineering*, 2nd Ed., Lewis Publishers, USA. 489pp.
- Fan, K.F., Kuo, M.C.T., Liang, K.F., Lee, C.S., Chiang, S.C., 2005. Interpretation of a well interference test at the Chingshui geothermal field, Taiwan. *Geothermics*, 34, 99-118.
- Huang, Y. C., Yeh, H. D., and Lin, Y. C., 2008. A computer method based on simulated annealing to identify aquifer parameters using pumping test data, *International Journal for Numerical and Analytical Methods in Geomechanics*, 32, 235-249, doi:10.1002/nag.623.
- Le Borgne, T., De Dreuzy, J. R., Davy, P., and Touchard, F., 2004. Equivalent mean flow models for fractured aquifers: Insights from a pumping tests scaling interpretation, *Water Resources Research*, 40, 10.1029/2003WR002436.
- Papadopoulos, I. S., 1965. Nonsteady flow to a well in an infinite anisotropic aquifer, *Proceeding of the Durbrovnik Symposium on the Hydrology of Fractured Rocks*, International Association of Scientific Hydrology, 21-31.
- Tong, L.T., Ouyang, S., Guo, T. R., Lee, C. R., Hu, K. H., Lee, C. L. and Wang, C. J., 2008. Insight into the Geothermal Structure in Chingshui, Ilan, Taiwan, *Terr. Atmos. Ocean. Sci.*, 19(4), 413-424.
- Yeh, H. D., Lin, Y. C., and Huang, Y. C., 2007. Parameter identification for leaky aquifers using global optimization methods, *Hydrological Processes*, 21, 862-872, doi:10.1002/hyp.6274.